A Hybrid Heartbeats Classification Approach Based on Marine Predators Algorithm and Convolution Neural Networks

ESSAM H. HOUSSEIN[1], **DIAA SALAMA ABDELMINAAM**[2,3], **IBRAHIM E. IBRAHIM**[4], **M. HASSABALLAH**[5], **AND YASER M. WAZERY**[1]

[1]Faculty of Computers and Information, Minia University, Minia 61519, Egypt
[2]Faculty of Computers and Artificial Intelligence, Benha University, Benha 12311, Egypt
[3]Faculty of Computers Science, Misr International University, Cairo 11341, Egypt
[4]Faculty of Computers and Information, Luxor University, Armant, Egypt
[5]Department of Computer Science, Faculty of Computers and Information, South Valley University, Qena 83523, Egypt

Corresponding author: Diaa Salama AbdElminaam (diaa.salama@fci.bu.edu.eg)

ABSTRACT The electrocardiogram (ECG) is a non-invasive tool used to diagnose various heart conditions. Arrhythmia is one of the primary causes of cardiac arrest. Early ECG beat classification plays a significant role in diagnosing life-threatening cardiac arrhythmias. However, the ECG signal is very small, the anti-interference potential is low, and the noise is easily influenced. Thus, clinicians face challenges in diagnosing arrhythmias. Thus, a method to automatically identify and distinguish arrhythmias from the ECG signal is invaluable. In this paper, a hybrid approach based on marine predators algorithm (MPA) and convolutional neural network (CNN) called MPA-CNN is proposed to classify the non-ectopic, ventricular ectopic, supraventricular ectopic, and fusion ECG types of arrhythmia. The proposed approach is a combination of heavy feature extraction and classification techniques; hence, outperforms other existing classification approaches. Optimal characteristics were derived directly from the raw signal to decrease the time required for and complexity of the computation. Precision levels of 99.31%, 99.76%, and 99.47% were achieved by the proposed approach on the MIT-BIH,EDB, and INCART databases, respectively.

INDEX TERMS Heart disorder classification, marine predators algorithm, deep neural networks, CNN, feature fusion.

I. INTRODUCTION

Cardiac arrhythmia, a disease characterized by irregular heart activity [1]–[3] and a cardiac condition associated with the rhythm of the heartbeat or heart rate, is the main source of cardiac mortality. It is reported that about 2200000 people in the US and 4500000 people in EU annually die from arrhythmia [4], which exceeds the mortality of all cancers combined. An arrhythmia is a concern with the rate or rhythm of the heartbeat. The heart may beat excessively quickly, too slowly or in an unaccountable rhythm during arrythmia. The disorder is called tachycardia when the heart beats too quickly. The condition is called bradycardia when a heart beats too slowly [5].

Various studies have been conducted using computer-aided detection (CADe) to precisely forecast arrhythmia in order

The associate editor coordinating the review of this manuscript and approving it for publication was Jenny Mahoney.

to enhance diagnostic efficiency [6]–[8]. Thus, This work aims to early alerts for unusual disorders may be given by creating a computational framework focused on machine learning that rapidly, correctly, and consistently diagnose cardiac arrhythmia such that qualified doctors can provide appropriate care. However, because of the variance of ECG signals and the changes in the recording environment, this is still a challenge for a computer to execute automatically. For a healthy person, even in a short time, morphology and rhythm may vary considerably. Many methods for generic heartbeat categorization with ECG-based signal were proposed. A fully-automatic approach to detect arrhythmia from signals collected by the electric cardiogram (ECG) system can be used in four phases: (1) ECG preprocessing signal (2) signal segmentation, (3) Features extraction and (4) classification. In each of the four steps, an action is taken, and the goal is to discriminate/classify the type of heartbeat [9], [10]. Different techniques have been extensively

investigated for preprocessing phase and features extraction phases [11]–[13].

The methods employed in the preprocessing step greatly influence and are selected as such for the final output. The results of the cardiac segmentation process in the instance of QRS detection are nearly optimal. While the subject of ECG delineation is essential, the methodologies studied here are only of little significance. Researchers have been led to optimize the accuracy level in numerous ways for ECG classification strategies, thus neural fuzzy networks [14], [15], genetic algorithms [9], Bayesian approaches [16], key component analysis based on support vector machine (SVM) [17], and key component analysis based on neural networks [18] have been suggested.

The main contributions of this paper are summarized as follows:

- An efficient architecture of deep CNN is designed. It folds four convolutional layers with two fully connected layer to improve the capacity of the CNN for ECG classification. The structure of the input data and convolution is revamped to satisfy the ECG classification process, where the input data is always in one dimension rather than multi-dimensions like traditional used input. Sub-sampling convolutional filters are adopted to extract more Plentiful features. We extended information about original heartbeat using different handcraft features (using different descriptors). The effectiveness and efficiency of deep CNN for ECG classification are evaluated.
- A new training mechanism based on MPA-CNN learning generic features and fine-tuning classification parameters to learn the characteristic of heartbeats is proposed for ECG classification (CNN for classification task and MPA algorithm for optimizing learning parameters). The MPA-CNN is trained based on a large common dataset containing Plentiful ECG heartbeats, which accelerates the convergence of the MPA-CNN. Moreover, MPA-CNN accelerates learning time and provide high accuracy percentage.
- We explore feature fusion and propose a novel scheme for combining CNN with handcrafted features. The scheme has two main advantages: First, handcraft features in CNN, which takes advantage of some robust and local features; second, discriminative handcrafted features help to improve the performance of original CNN and accelerate training time.
- The available ECG datasets highly category imbalanced as regular heartbeats take place much more often than irregular heartbeats (over sampling for regular and under sampling for irregular), resulting in the majority of methods providing low sensitivity and positive predictive values for heartbeats classification. To solve the problem of imbalanced category classification, synthetic minority over sampling technique (SMOTE) is used for over sampling and Random under sampling for under

sampling both are applied over the extracted handcraft features.
- Several experiments are conducted on common benchmarking datasets, where the obtained results demonstrate the effectiveness of the proposed approach. The state-of-the-art performance is achieved using the MPA-CNN, and the events of VEB and SVEB can be identified accurately.

The rest of the paper is organized as follows. Section II discusses the related works. Section III is devoted to present the preprocessing methods applied to filter and segment the ECG signals, feature extraction methods, the CNN architecture, the MPA algorithm, and the benchmarking datasets. Section IV explains the proposed MPA-CNN approach that combines CNN architecture with MPA to enhance the ECG arrhythmia classification. Section V provides the experimental results and comprehensive evaluation of the proposed MPA-CNN approach compared with other well-known metaheuristic algorithms. Finally, Section VI concludes the paper.

II. RELATED WORK

Simulated linear and nonlinear properties have been derived and classified by Lee *et al.* [19]. They categorized coronary artery diseases using various classifier forms. This classification was conducted using metaheuristic optimization techniques, such as nature, optimization of particle swarm (PSO) [20], Henry gas solubility optimization (HGSO) [21], Harris hawks optimization (HHO) [22], [23], Marine Predators Algorithm (MPA) [24], Barnacles Mating Optimizer (BMO) algorithm [25], Tunicate Swarm Algorithm (TSA) [26], Gradient-Based Optimizer (GBO) [27], Turbulent Flow of Water-Based Optimization (TFWBO) [28], [29], Owl search algorithm (OSA) [30], Fitness-Dependent optimizer (FDO) [31], Squirrel Search Algorithm (SSA) [32], and Deep Learning methods [33]–[35]. In [36], the discrete wavelet transform (DWT) performance and SVM coronary heart diseases, decision tree (DT), K-nearest neighbor, and neural network probability classifiers were compared to identify normal and nonlinear techniques. One of the most useful nature-inspired optimization algorithms referred to as bacterial-foraging-optimization (BFO) was developed by Kora *et al.* [37]. The BFO modifications with SVM on the MIT-BIH dataset produced precision levels of 98.9% and 99.3%. A compression algorithm based on DWT and PSO was used to generate ECG.

A PSO one-dimensional CNN with SVM (1D CNN-SVM) architecture was proposed by Navaneeth *et al.* [38] for real-time disease detection and classification. The efficiency of the proposed architecture was validated with a novel hardware model to detect chronic kidney disease (CKD) from saliva samples. The urea content of the samples was tracked to detect CKD by converting urea into ammonia. On hydrolysis, the urea produces ammonia in the presence of the urease enzyme. The output of the architecture was optimized using a PSO algorithm to control the parameter

values. The proposed design outperforms existing traditional methods since this method is a synthesis of heavy feature extraction and classification techniques. Optimal characteristics were derived directly from the raw signal to decrease the time required for and complexity of the computation. A precision of 98.255% was attained for the suggested architecture. While, Zubair *et al.* [39] proposed an ECG beat recognition method using CNN. The MIT-BIH arrhythmia data collection was used in the analysis, and five Association for the Advancement of Medical Instrumentation (AAMI) groups were identified. An accuracy of 92.7% was attained. In [40], an automatic classification scheme was proposed based on a deep learning (DL) methodology to control and diagnose cardiac disease (CD). For an unsupervised type of feature learning and deep neural networks (DNNs) as a classifier, the proposed DL architecture is divided into deep auto-encoders (DAEs). However, DL generates an embedded function extraction and feature selection directly from raw data in DAE pretraining and DNN fine-tuning processes. DAEs will derive high-level functionality from training data and also from unknown data. Ten classes of imbalanced data from ECG signals are used in the proposed model. An abnormality is commonly considered for early CD diagnosis since CD is associated with the heart area. The model is compared with the shallow models and the DL methods to verify the result. The results showed that with 99.73% precision, 91.20% sensitivity, 93.60% precision, 99.80% specificity, and a 91.80% F1 score, the proposed approach achieved a promising efficiency.

In [41], a DL approach incorporating CNNs and long-term memory networks (LSTM) is suggested to automatically classify six forms of ECG signals: regular (N) sinus rhythm parts, atrial fibrillation, ventricular bigeminy (B), atrial flutter (AFL), pacing rhythm (P), and sinus bradycardia (SBR). A multi-input structure for processing 10 s ECG signal segments and corresponding RR intervals from the MIT-BIH arrhythmia dataset was added to the proposed network. This network reached 99.32% accuracy with a five-fold cross-validation approach. Using the sparse representation methodology to effectively represent the various ECG signals for efficient analysis. Raj and Ray [42] proposed a new feature extraction technique. Four features were extracted, such as time delay, frequency, width parameter, and expansion coefficient square. These features were concatenated and analyzed to evaluate the optimal length of the racially discriminatory feature vector representing each of the ECG signals. These extracted features representing the ECG signals were further categorized using machine learning techniques, such as k-NN, SVM, RBFNN, and PNN. Besides, the classifiers' learning parameters were optimized using ABC and PSO techniques.

III. PRELIMINARIES AND DATASETS
The ECG is a non-invasive, affordable monitoring instrument used to track the heart's electrical function and is commonly used in various applications [43]. The ECG output
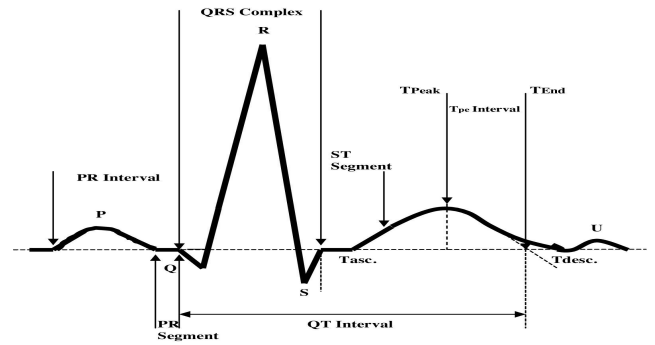
FIGURE 1. Fiducial points and different regular intervals of a heartbeat (waves).

is described by electrical power in the form of signals that represent the heart's electrical operation over some time. These signals consist of essential physiological data that are commonly used for heartbeat function research. The heart's electric field is created by placing an electrode on different parts of the body [44]. ECG signals are created in three wave sequences: the P wave, the QRS waves (known as the QRS complexes), and the T wave, which are transmitted regularly over time and comprise a periodic signal as shown in Fig. 1.

A fully automated method for the identification of arrhythmias from signals obtained by an ECG system can be divided into four steps: (1) ECG signal preprocessing, (2) heartbeat segmentation, (3) feature extraction, and (4) classification [37]. An action is taken in each of the four steps, and the final goal is to discriminate/identify the type of heartbeat. For ECG signal preprocessing as a first step, filter techniques remove distracting elements from the digital ECG data, such as power line interference and baseline drift [45]. Signal denoising enhances the efficiency of the proposed classification model. The FIR band-pass with [0,5; 50] Hz spectrum is used [46]. A linear band-pass filter, with a c = [F-Low = 0.5; F-High = 50] cut-off frequency(F), has therefore to be applied.

A. FEATURES EXTRACTION
The pre-trained CNN accepts RGG images, whereas the ECG signals are raw vector. To tackle this drawback, a 1D CNN has been proposed. Although CNNs have achieved excellent success in ECG classification tasks but, handcrafted features still play important roles such as the global information for the signal and R-R intervals where the single heartbeat interval does not include the distance values for the adjacent beats(see section III-A6). Handcrafted features are designed to define heartbeat content from particular aspects, and can provide additional information for CNN on ECG classification tasks. The extraction of features is performed as follows. The R-peak annotations provided with the MIT-BIH, EDB, and INCART datasets are used as a reference point for the segmentation and identification of beats. For each beat, a window of size 200 ms is centered around the R-peak 80 ms

before and 120 ms after the peak, and all the features inside that region are then computed using the following descriptors.

1) 1D-LOCAL BINARY PATTERN
The 1D-LBP feature extraction descriptor is employed in this work to gather valuable knowledge about the ECG signal. [47]. The foundation of the original 2D version is preserved in the adapted 1D version, which is characterised as an ordered collection of binary comparisons between the centre value and its nearby values. In addition, a histogram with the frequency of each binary pattern is created. Using a 1D uniform LBP technique, the raw ECG signal is first translated into the LBP domain, with the eight surrounding samples forming a 59-dimensional description.

2) HERMITE BASIS FUNCTION (HBF)
ECG signals (i.e., the accompanying QRS complexes) have a structure commensurable to Hermite waves. Hermite functions can be habituated to estimate these signals with the fewest coefficients possible while maintaining precision. Fitting of 3,4, and 5-degree Hermite polynomials yielded the coefficients [48].

3) HIGHER ORDER STATISTICS (HOS)
The quest for trustworthy criteria that give the best ECG heartbeats is the key difficulty in classifying it. To gather attributes for effective classification, higher-order statistics (HOS) have been widely used [49]. Kurtosis is utilized to estimate the deviation of a distribution from a Gaussian distribution, which is the substratum of HOS. However, Kurtosis is associated with a high-frequency QRS transition. Skewness implicatively insinuates a non-Gaussian pattern in the probability distribution of a signal and describes a feature that defines smooth transitions during QRS onset and offset [50].

4) CENTRAL MOMENT
This is a popular quantitative measure of the form that characterises a group of points. Because of its tight sodality with these factors, it is widely used to determine skewness and kurtosis coefficients. The fifth moment is utilised in feature extraction to detect and define key features (such the R-beaks) in an ECG signal, as well as to quantify the symmetry of the input data.

5) DISCRETE WAVELET TRANSFORM (DWT)
The essential properties of the ECG signal are well represented by DWT. Daubechies and Sweldens [51] used a wavelet with (db1) function characterized by three decomposition levels to extract a set of features.

6) R-R INTERVALS
R-R intervals are typically used for feature extraction in the classification of ECG signals. Different R–R intervals occur between any consecutive beats.

- Pre-RR: the distance between the current heartbeat and the previous beat.
- Post-RR: the distance between the current heartbeat and the following beat.
- Local-RR interval: the average of 10 previous Pre-RR values.
- Global-RR: containing the average of the Pre-RR values produced in the last 20 min.
- A normalized version of previous intervals is computed;

B. BENCHMARKING DATASETS
Various well-known Physionet-based datasets, such as the MIT-BIH, EDB, and INCART datasets, were used to train and test the suggested algorithms against the most recently available methodologies.

1) MIT-BIH ARRHYTHMIA DATASET (MIT-BIH)
The MIT-BIH dataset is a freely accessible dataset with regular investigation content for heart rhythm detection from 47 individual patients. This dataset has 48 records (each with a period of 30 minutes and a sample rate of 360 Hz), and the data is properly annotated. Two signals are recorded in the dataset: a bipolar limb lead known as modified-lead (MLII) and unipolar chest leads known as V leads (V1, V2, V3, V4, V5, and V6). The MLII-type record provides a perfect view of all significant waves, including Q-waves, P-waves, R-waves, T-waves, and S-waves, and may thus be shared across all recordings.

2) EUROPEAN ST-T DATASET (EDB)
For the application of ST and T-wave designs, the EDB was used. This collection contains 90 annotated samples corresponding to 79 participants' outpatient ECG data. Each recording lasts two hours, with two signals recorded at 250 samples per second.

3) ST. PETERSBURG INCART DATASET (INCART)
INCART is a 12-lead arrhythmia dataset made up of 75 annotated recordings extracted from 32 Holter records. Each record is 30 minutes long and has 12 regular leads sampled at 257 Hz each. Patients receiving coronary heart disease tests provided the initial data. Considering the recommended practice of the AAMI for all used datasets, classes forms are divided into five categories. For each recording, only one channel is used for the classification task.

4) IMBALANCE CLASS
Unbalance class variance represents the non-uniformity of the class labels. Several instances occur in one class and a few occur in other classes [52]. Class inequality is a critical issue encountered in various fields, such as bioinformatics [53], textual classification [54], and health diagnosis [55]. To solve the problem of imbalanced category classification, a synthetic minority oversampling technique (SMOTE) is used for oversampling and random undersampling for undersampling are

both applied in the features set. Random undersampling: is a re-sampling technique that generates a random sub-sample of majority class instances. SMOTE: is a popular oversampling method proposed by Chawla *et al.* [56]. The main objective of this approach is to produce "synthetic" minority samples instead of duplicating the samples. In this study, SMOTE and random undersampling are selected to obtain an improved class distribution balance.

5) DATASET DIVISION
The AAMI standard defines the protocol for examining and analyzing arrhythmia classification methods. It also defines which datasets should be used. However, it does not specify which patients/heartbeats should be used to create the model to be classified (training phase) and which patients/heartbeats should be used for the evaluation methods (i.e., the testing phase). So there is different such inter-patient, intra-pathion, semi-automatic, and fully-automatic approaches. In this regard, de Chazal *et al.* [57] have found that the use of heart beats from the same patient for both learning and testing is a bias in the evaluation process. In order to define a protocol, de Chazal *et al.* [57] suggested a partition of the heartbeats from the MIT-BIH dataset only. The first collection consists of all the heart beats of the records:101, 106, 108, 109, 112, 114, 115, 116, 118, 119, 122, 124, 201, 203, 205, 207, 208, 209, 215, 220, 223 and 230, called Dataset 1 (DS1). While the second is composed of all heartbeats of records: 100, 103, 105, 11, 113, 117, 121, 123,200, 202, 210, 212, 213, 214, 219, 221, 222, 228, 231, 232, 233 and 234, called Dataset 2 (DS2). But this division has several issues that were previously connected to Mar *et al.* [58] and Llamedo & Martinez [59].

The imbalance between groups prompted the writers to add two reports of the same patient to the two sets already listed. Although these documents, 201 and 202, are from the same patient and belong to the DS1 and DS2 collections, the outcomes may be marginally higher than expected. In comparison, records 201 and 202 are greatly clustered in a substantial portion of the SVEB heartbeats class. The use of the imbalanced record 232 in DS2 is another major limitation of the protocol suggested in [57]. This record includes more than 75% of the heart beats of the SVEB class. As such, techniques that obtain the right classification of the heartbeat of this record can be mistakenly treated as state-of-the-art, when in fact they may only be specialized in the heartbeat of a single patient. In the other hand, some researchers use semi-automatic approaches [60], [61] to boost the recorded performance. Semi-automatic methods will boost results by more than 40% even though a limited number of heart beats are chosen for adaptation. The downside to such methods is that they need the participation of specialists. Our approach follows fully automated methods in which heartbeats are automatically chosen for the training and testing phase. K-fold with k = 5 splitting strategy for obtaining training, validation and testing sets in automatic manner.

C. CONVOLUTIONAL NEURAL NETWORK
In this paper, an architecture is designed to provide high recognition output on a CNN-based ECG (MII) lead, which has been configured to include uncomplicated and typical CNN layers. Fig. 2 shows a block diagram of the 10-layer deep CNN model. The ECG beats are fed into the model through the input layer. Sequentially, each beat passes through ordered convolution and max-pooling layers and converts these into function maps of different sizes. An automatic prediction of classes is provided for the dense layer by studying these feature maps. A dropout technique is used to avoid overfitting during model training.

D. MARINE PREDATORS ALGORITHM
Similar to most of the metaheuristics, MPA is a nature-inspired heuristic algorithm that mimics predator behavior when attacking prey. Predators employ two techniques (namely Brownian and Levy motion) when targeting their prey. For a balance between the two approaches, predators calculate the velocity ratio from the prey to their current position [62]. The mathematical model describing these techniques is formulated as follows:

1) INITIALIZATION
Like most of the metaheuristic algorithms, MPA starts with the initial solution, which is uniformly distributed over the search space:

$$X_0 = X_L + \text{rand} \ (X_U - X_L) \tag{1}$$

where X_L and X_U are the maximum and minimum limits or boundary for search spaces while the rand is a unified random vector in the range 0 to 1.

2) ELITE AND PREY MATRIX CONSTRUCTION
The top predator is the best one for the foraging cycle based on the survival of the fittest principle, and this predator is used to create an $n \times d$ Elite matrix that is denoted as E.

$$E = \begin{bmatrix} X_{1,1}^I & X_{1,2}^I & \cdots & X_{1,d}^I \\ X_{2,1}' & X_{2,2}^I & \cdots & X_{2,d}' \\ \vdots & \vdots & \vdots & \vdots \\ X_{n,1}^I & X_{n,2}^I & \cdots & X_{n,d}^I \end{bmatrix} \tag{2}$$

where $\vec{X^I}$ denotes the best predator vector, which is repeated n times to create the matrix. n and d refer to the number of search space agents and the dimensions, respectively.

Another matrix with the same dimension as Elite is referred to as Prey and the predator positions are updated based on this matrix.

$$Py = \begin{bmatrix} X_{1,1} & X_{1,2} & \cdots & X_{1,4} \\ X_{2,1} & X_{2,2} & \cdots & X_{2,d} \\ X_{3,1} & X_{3,2} & \cdots & X_{3,d} \\ \vdots & \vdots & \vdots & \vdots \\ \vdots & \vdots & \vdots & \vdots \\ X_{n,1} & X_{1,2} & \cdots & X_{n,d} \end{bmatrix}_{nxd} \tag{3}$$

Column 1

Input layer		EDB / INCART	MIT-BIH
	Input	117	127
	Output	117	127

Conv 1D		EDB / INCART	MIT-BIH
	Input	117	127
	Output	(113,32)	(123,32)

Conv 1D		EDB / INCART	MIT-BIH
	Input	(113,32)	(123,32)
	Output	(111,64)	(123,164)

MaxPooling 1D		EDB / INCART	MIT-BIH
	Input	(111,64)	(123,64)
	Output	(55,64)	(60,64)

DropOut		EDB / INCART	MIT-BIH
	Input	(55,64)	(60,64)
	Output	(55,64)	(60,64)

Column 2

Conv 1D		EDB / INCART	MIT-BIH
	Input	(55,64)	(60,64)
	Output	(43,128)	(48,128)

Conv 1D		EDB / INCART	MIT-BIH
	Input	(43,128)	(48,128)
	Output	(37,256)	(42,256)

MaxPooling 1D		EDB / INCART	MIT-BIH
	Input	(37,256)	(42,256)
	Output	(36,256)	(41,256)

Flatten		EDB / INCART	MIT-BIH
	Input	(36,256)	(41,256)
	Output	9216	10496

Full connectivity		EDB / INCART	MIT-BIH
	Input	9216	10496
	Output	128	(123,164)

Column 3

Full connectivity		EDB / INCART	MIT-BIH
	Input	128	128
	Output	128	128

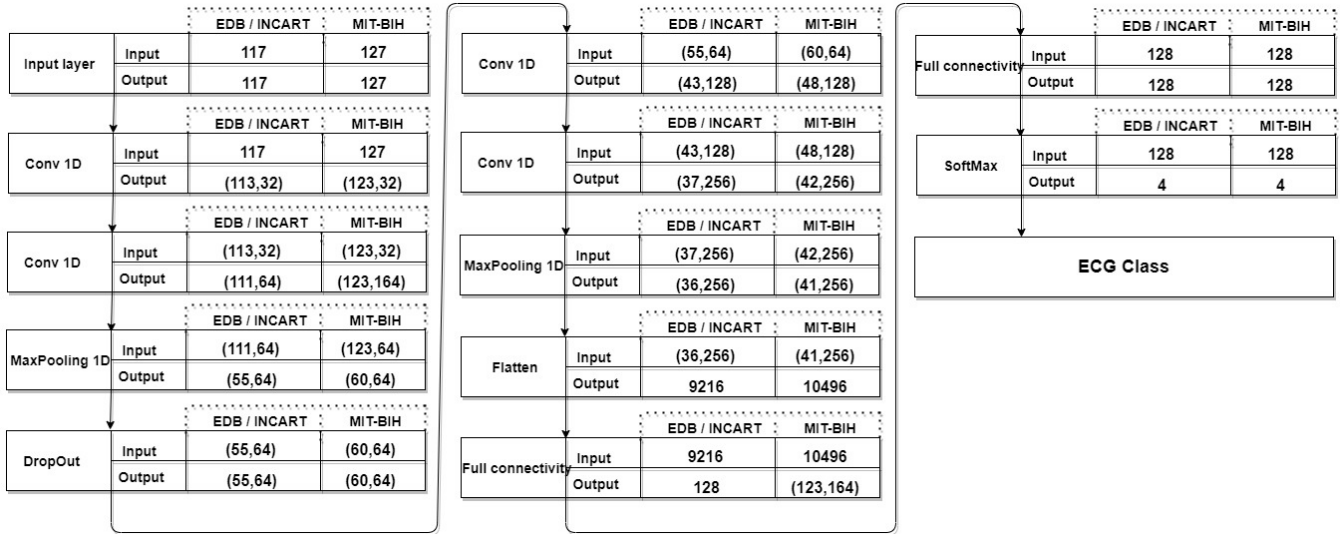| SoftMax		EDB / INCART	MIT-BIH
	Input	128	128
	Output	4	4

ECG Class

FIGURE 2. Block representation of the proposed CNN model.

These two metrics are the fundamental parameters of the optimization process where the initialization stage creates the initial Prey and the corresponding best fit predator creates the Elite matrix.

3) OPTIMIZATION PROCESS

In the optimization cycle, the predators seek a better optimal solution than the current solution. The MPA optimization method is mathematically formulated as follows:

In the first step, which is the discovery phase, predators seek to move faster (than previously) before they locate their prey as the essence of all metaheuristic algorithms at the beginning of the optimization procedure. This phase is formulated as follows:

$$\text{while } t < \frac{1}{3} * t_{\max}$$

$$\vec{stepsize}_i = \vec{R}_L \otimes \left(\vec{E}_i - \vec{R}_L \otimes \vec{py}_i \right) \tag{4}$$

$$\overrightarrow{Py}_i = \overrightarrow{Py}_i + P \cdot R \otimes stepsize_i \tag{5}$$

where $\vec{R}_L$ is a vector of random values based on the Levy distribution representing Levy movements. Multiplication of $\vec{R}_L$ and Elite follows the predator's movements in the Lévy approach [63]. Applying the phase size to the Elite location simulates the predator's movements; thus, updating the prey location. Given that the step size of the Levy distribution is mainly correlated with small steps, this section helps the exploitation stage. In the middle step, MPA splits the population into two sections to differentiate between exploration and exploitation; the former will be modified using the Brownian method while the latter will be considered using the Lévy method. The mathematical model in this step is given as follows: While $\frac{1}{3} * t_{\max} < t < \frac{2}{3} * t_{\max}$ For the first half of the population:

$$\vec{stepsize}_i = \vec{R}_L \otimes \left(\vec{E}_i - \vec{R}_L \otimes \vec{py}_i \right) \tag{6}$$

$$\vec{py}_i = \vec{py}_i + P * \vec{R} \otimes \vec{stepsize}_i \tag{7}$$

For the second half of the population:

$$\vec{stepsize}_i = \vec{R}_B \otimes \left(\vec{R}_B \otimes \vec{E}_i - \vec{P}_i \right) \tag{8}$$

$$\vec{py}_i = \vec{E}_{i_i} + P * CF \otimes \vec{stepsize}_i \tag{9}$$

where, CF is a parameter updated based on the iterations to control the step size and is generated by the following equation:

$$CF = \left(1 - \frac{t}{t_{\max}} \right)^{\left(2\frac{t}{t_{\max}} \right)} \tag{10}$$

For the final phase of the optimization process, the population can only be modified using the Levy flight as follows: While it $> \frac{2}{3} * \max\_iter$

$$\vec{stepsize}_i = \vec{R}_L \otimes \left(\vec{R}_L \otimes \vec{E}_i - \vec{py}_i \right) \tag{11}$$

$$\vec{py}_i = \vec{E}_i + P * CF \otimes stepsize_i \tag{12}$$

Based on the nature of the predators associated with the surrounding environments, sharks spend more than 80% of their time near FADs [64]. For the remaining 20%, sharks will take a longer jump (than that corresponding to 80% of the time) in different dimensions probably to find an environment with another prey distribution. The FADs effect is mathematically expressed as follows:

$$\vec{py}_1 = \begin{cases} \vec{py}_1 + cF \left[\vec{x}_L + R \otimes \left(\vec{x}_U - \vec{x}_L \right) \right] \\ \quad \otimes \vec{U} \text{ if } r < FADS \\ py_i + [FADS(1 - r) + r] \left(\vec{py}_{r1} - \vec{py}_{r2} \right) \\ \quad \text{if } r > FADS \end{cases} \tag{13}$$

where, r is a number randomly generated in the range of [0, 1]. $FADs = 0.2$ indicates the influence of FADs on the updating process.

Marine predators have a good memory of successful foraging sites. This capability is simulated by memory saving in MPA, and the process improves the solution quality with the progress of iteration. After upgrading the Prey effect and applying the FADs effect, this matrix is tested for Elite Upgrade Fitness. The fitness of the solution in the current iteration is compared with the fitness in the previous iteration; however, if more suitable, the new one substitutes the solution.

1: Initialization Step, P, TP, TF, Py_i.
2: **while** $t < t_{max}$ **do**
3:     Compute the fitness value of each $\overrightarrow{py}_i, f\left(\overrightarrow{py}_i\right)$
4:     Construct E
5:     implement the memory saving
6:     Update CF based on Eq. 10
7:     **for** each py_i **do**
8:       **if** $\left(t < \frac{1}{3} * t_{\max}\right)$ **then**
9:         Reposition the current $\overrightarrow{py}_i$ based on Eq. 5
10:       **else**
11:         **if** $\left(\frac{1}{3} * t_{\max} < t < \frac{2}{3} * t_{\max}\right)$ **then**
12:           **if** $\left(i < \frac{1}{2} * n\right)$ **then**
13:             Reposition the current $\overrightarrow{py}_l$ according to Eq. 7
14:           **else**
15:             Reposition the current $\overrightarrow{py}_i$ according to Eq. 9
16:           **end if**
17:         **else**
18:           Reposition the current $\overrightarrow{py}_i$ according to Eq. 12
19:         **end if**
20:       **end if**
21:     **end for**
22:     Compute the fitness value of each $\overrightarrow{py}_i, f\left(\overrightarrow{py}_i\right)$
23:     Update $TopPradatorPos$, and $TopPredatorFit$.
24:     Apply the memory saving
25:     Apply the FADS for $\forall$ py $_i$ based on Eq. 13
26:     $t++$
27: **end while**

IV. THE PROPOSED MPA-CNN APPROACH

Fig. 2 shows the CNNs architecture used in the proposed method, where it is consist of an input layer that will be processed using 2 convolution kernel with size 5×5 and 3×3, 2 sub-sampling kernel with size 2×2 pixels, 2 convolution kernel with size 5×5 and 3×3, 2 subsampling kernel with size 2×2 pixels, 2 full connection fully connected layer and the last layer is the soft-max. The proposed method process can be seen on Fig. 3. MPA in this work would optimize learning rate parameter. To calculate the fitness value, the root mean square error between prediction labels vector and the true labels vector. In general, the flow of the proposed method contains of different procedures as shown below: 1) the first one is initializing the learning rate of the CNN in the range of $1e^{-7}$ to 1. The batch size of CNN is 32, the number of CNN epoch value is 6 but early stopping is used to specify an
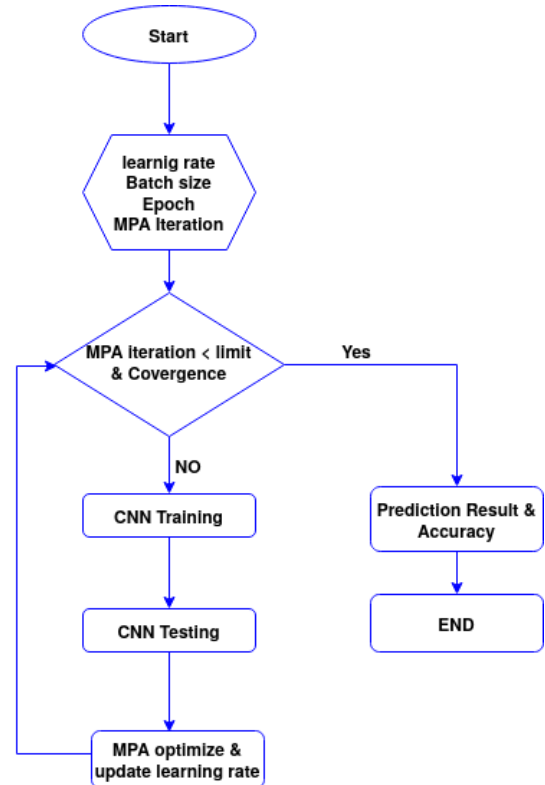

FIGURE 3. Flowchart of the proposed MPA-CNN method.

arbitrary large number of training epochs and stop training once the model performance stops improving on a k-fold validation dataset. To adjust the best value for classification process k-fold with $k = 5$ strategy is used. MPA iteration limit is 100. The convergence status of MPA issued to check the convergences of MPA, if the error value has not changed for ten iterations, then the MPA is considered as convergent; 2) after setting up the experiment, the next step is run CNN training process. 3) the learning rate value will be update if the solution of search agent has less error compare with old learning rate value; 4) the MPA will run as long as the iteration number of MPA and the convergence solution have not satisfied; 5) after the CNN Training, the model will be tested 6) the result of test is accuracy of CNN, it represent how precise of the model can predict the actual value of testing dataset. The overall framework consists of the initialization step, evaluation step, and updating, and memory saving steps as shown in Fig. 4.

A. PARAMETERS OPTIMIZATION

Tuning parameters for a machine learning methodology significantly affect the classification efficiency. The learning rate is a hyperparameter that controls how much the model can adjust in response to the expected error each time the model weights are changed. Choosing a learning rate is difficult, since a value that is too small can result in a lengthy training phase that may stall, whereas a value that is too high could result in learning a sub-optimal range of weights that is too fast or an unpredictable training process. From Fig. 5 if
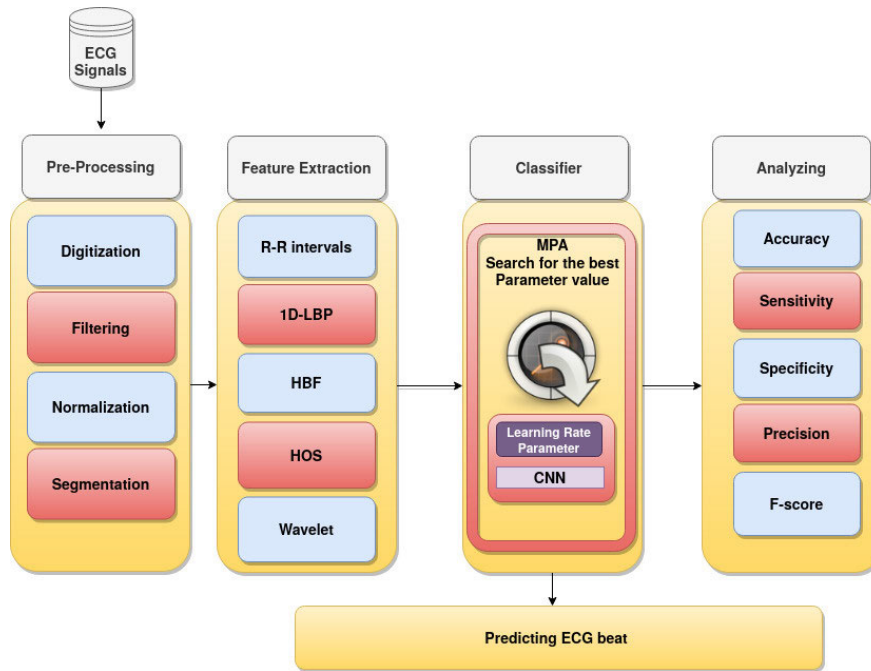
FIGURE 4. The general framework of the proposed MPA-CNN approach.
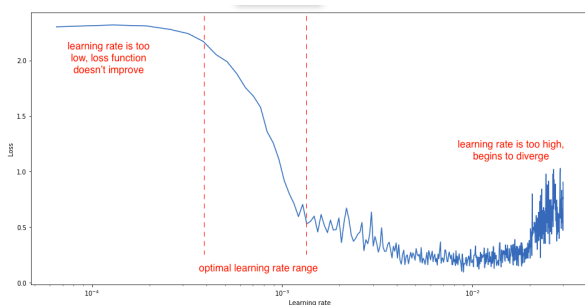

FIGURE 5. Three phases for different learning rates.

the learning rates which are too low, the loss may decrease, but at a very shallow rate. When entering the optimal learning rate zone, you'll observe a quick drop in the loss function. A further increase in the learning rate would cause the loss to increase as the parameter changes cause the loss to "bounce around" and even diverge from the minimum. The MPA algorithm try to optimize the initial learning rate parameter to fit in the optimal area. MPA select a value between $1e^{-7}$ and 1.

B. FITNESS FUNCTION

The fitness function is a mathematical equation that evaluates the effectiveness of a particular task's solution. One of the most critical challenges in developing an optimization algorithm is to choose the required fitness role. In this study, the root mean square error for the classification is chosen via the search process as the solution criterion. The root mean square error between prediction labels vector (Y) and the true labels vector (X). MPA optimization is done by minimized the

TABLE 1. Confusion matrix.

	Classified X	Classified Y
Actual X	True positive (Tp)	False negative (Fn)
Actual Y	False positive (Fp)	True negative (Tn)

root mean square error.

$$Rmse = \sqrt{(\frac{1}{n}) \sum_{i=1}^{n} (y_i - x_i)^2} \qquad (14)$$

V. EXPERIMENTS RESULTS AND DISCUSSION
A. PERFORMANCE METRICS
The proposed MPA-CNN model is evaluated using the following standard criteria: (1) accuracy, (2) precision, (3) specificity, (4) sensitivity, and (5) F1 score. The performance metrics typically relied on different major metrics (positive/negative/true/false) of a binary classification test.

let define two possible predicted classes: X and Y. Thus, Tp are positive instances classified as positive, Fn are positive instances classified as negative, Fp are negative instances classified as positive, Tn are negative instances classified as negative, see Table 1. Based on the confusion matrix, while there is a multi-class confusion matrix of the form

$$C = \text{Actual} \begin{matrix} & \text{Classified} \\ c_{11} & \cdots & c_{1n} \\ \vdots & \ddots & \\ c_{n1} & & c_{nn} \end{matrix} \qquad (15)$$

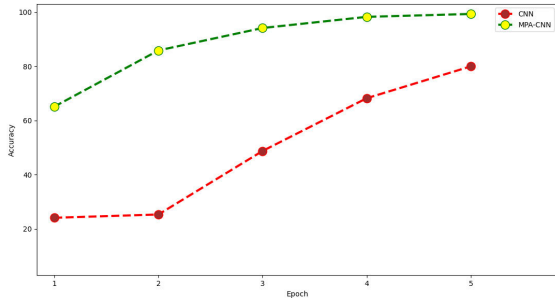The confusion elements for each class are given by:

$$Tp_i = c_{ii}$$
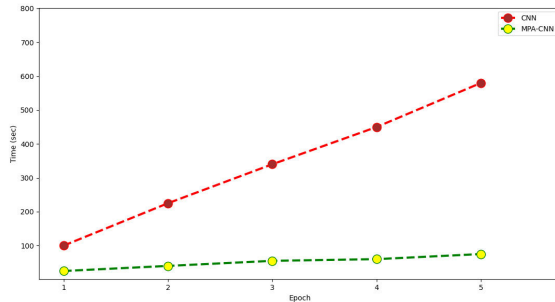
FIGURE 6. Accuracy optimization on MIT-BIH.

FIGURE 7. Learning time optimization on MIT-BIH.

$$Fp_i = \sum_{l=1}^{n} c_{li} - Tp_i$$

$$Fn_i = \sum_{l=1}^{n} c_{il} - Tp_i$$

$$Tn_i = \sum_{l=1}^{n}\sum_{k=1}^{n} c_{lk} - Tp_i - Fp_i - Fn_i$$

$$ACC_i = \frac{TP_i + Tn_i}{Tp_i + Fn_i + Fp_i + Tn_i}$$

$$ACC = \frac{1}{n}\sum_{i=1}^{n} ACC_i \qquad (16)$$

The total number of runs required for the MPA is set to be 30 runs and the following formulas describe the performance evaluation metrics.

- Average accuracy (AVG_{Acc}): (ACC) represents the accurate number of correspondences between the label of the sample data and the output of the classifier. It involves calculating the accuracy of each class separately and then averaging the results; thus, the average accuracy AVG_{Acc} is calculated from the best prey (At minimum value for the root mean square error over 100 iterations) as follows:

$$AVG_{Acc} = \frac{1}{N_r}\sum_{k=1}^{N_r} ACC_{best}^{(k)} \qquad (17)$$

where $N_r = 30$ is the total number of runs, n is the number of classes and $ACC_{best}^{(k)}$ best accuracy over 100 iterations.
- Average sensitivity (AVG_{Sn}): The sensitivity (Sn), which is used to assess the rate of prognosticating positive

samples, involves computing the sensitivity of each class separately and then averaging the results, determined as follows:

$$Sn_i = \frac{Tp_i}{Tp_i + Fn_i}$$

$$Sn = \frac{1}{n}\sum_{i=1}^{n} Sn_i \qquad (18)$$

The AVG_{Sn} is calculated from the best prey using the following equation:

$$AVG_{Sn} = \frac{1}{N_r}\sum_{k=1}^{N_r} Sn_{best}^{(k)} \qquad (19)$$

- Average specificity (AVG_{Sp}): The specificity (Sp) indicates the rate of prognosticating negative samples. It involves calculating the specificity of each class separately and then averaging the results as follows:

$$Sp_i = \frac{Tn_i}{Fp_i + Tn_i}$$

$$Sp = \frac{1}{n}\sum_{i=1}^{n} Sp_i \qquad (20)$$

The AVG_{Sp} is determined as follows:

$$AVG_{Sp} = \frac{1}{N_r}\sum_{k=1}^{N_r} Sp_{best}^{(k)} \qquad (21)$$

- Average Precision (AVG_{Pr}): The Precision (Pr), which is used to evaluate the classification approach effectiveness, involves computing the precision of each class separately and then averaging the results as given below:

$$Pr_i = \left\{ \frac{TP_i}{TP_i + FP_i} \right\}$$

$$Pr = \frac{1}{n}\sum_{i=1}^{n} Pr_i \qquad (22)$$

The AVG_{Pr} is determined as follows:

$$AVG_{Pr} = \frac{1}{N_r}\sum_{k=1}^{N_r} Pr_{best}^{(k)} \qquad (23)$$

- Average F1 score (AVG_{F1}): The F1 score ($F1$) is a measure of the test accuracy. It involves calculating the precision of each class separately and then averaging the results as shown below:

$$F1_i = \left\{ \frac{TP_i}{TP_i + FP_i} \right\}$$

$$F1 = \frac{1}{n}\sum_{i=1}^{n} F1_i \qquad (24)$$

The AVG_{F1} is determined as follows:

$$AVG_{F1} = \frac{1}{N_r}\sum_{k=1}^{N_r} F1_{best}^{(k)} \qquad (25)$$

TABLE 2. Performance analysis of the MPA-CNN model on the MIT-BIH dataset classes.

Classes	Accuracy(%)	Sensitivity(%)	Specificity(%)	Precision(%)	F − score(%)
N	99.14	98.55	99.33	98.01	98.28
S	99.59	99.0	99.79	99.37	99.19
VEBs	99.25	98.65	99.45	98.36	98.5
F	99.31	98.25	99.67	98.99	98.62
Average	99.32	98.61	99.56	98.68	98.65

TABLE 3. Performance analysis of the MPA-CNN model on the EDB dataset classes.

Classes	Accuracy(%)	Sensitivity(%)	Specificity(%)	Precision(%)	F − score(%)
N	99.70	99.19	99.87	99.60	99.39
S	99.74	99.74	99.74	99.24	99.48
VEBs	99.78	99.67	99.86	99.58	99.62
F	99.81	99.67	99.86	99.58	99.62
Average	99.76	99.49	99.85	99.55	99.51

TABLE 4. Performance analysis of the MPA-CNN model on the INCART dataset classes.

Classes	Accuracy(%)	Sensitivity(%)	Specificity(%)	Precision(%)	F − score(%)
N	99.25	98.22	99.59	98.78	98.50
S	99.61	99.52	99.63	98.91	99.21
VEBs	99.24	97.96	99.66	98.98	80.46
F	99.79	99.86	99.76	99.29	99.57
Average	99.47	98.89	99.66	98.99	94.44

The proposed model is trained and tested with ECG signals from three different datasets. The classification system is highly efficient for the trained and tested signals. The average accuracy of the proposed system is 99.32%, 99.76%, and 99.47% due to the maximum number of layer formation with the ECG signals from the datasets and optimization learning rate parameter using the MPA algorithm. The optimization evolution is stopped after 100 generations. Thus, merging the MPA and proposed CNN model allows the net to yield better diagnostic accuracy than that of the individual models. It enhances the model functionality in classifying cardiac signals of varying sequence lengths.

Fig. 6 and Fig. 7 show accuracy, time and its variance, when learning 5 epoch, the MPA-CNN are more accurate than base CNN. In addition to the MPA-CNN model has lower learning time than CNN, this suggests that the MPA-CNN has found parameter that can be successfully learned through optimization and has obtained good results. Also, the average optimization calculation time for MPA-CNN is 2547s. According to Tables 2, 3, and 4, all measures are higher than 97.96%. For the class level, the values of ACC and Sn are very high for all datasets (ACC > 99.14%, Se > 97.96%). The model classification accuracy is significantly improved and nearly balanced for all classes. The best and worst accuracy are for class F (improvement of 99.81% over that of the EDB dataset) and class N (improvement of 99.14% over that of the MIT-BIH dataset), respectively. A maximum of $\leq 0.41\%$ of the S class and $\leq 0.76\%$ of the VEB class were misclassified. The results for the S and VEB classes are very promising and indicate improvements over similar existing studies. It is worth noting that the AAMI recommended measures focus on the classification of S and VEB class heartbeats.

TABLE 5. Summary of the classification results obtained for the CNN and MPA-CNN on the MIT-BIH dataset.

Measures	CNN(%)	MPA-CNN(%)	Improvement(%)
AVG_{Acc}	93.95	99.32	5.37
AVG_{Sn}	87.03	98.61	11.58
AVG_{Sp}	96.28	99.56	3.28
AVG_{Pr}	89.22	98.68	9.46
AVG_{F1}	87.85	98.65	10.8

TABLE 6. Summary of the classification results obtained for the CNN and MPA-CNN on the EDB dataset.

Measures	CNN(%)	MPA-CNN(%)	Improvement(%)
AVG_{Acc}	97.66	99.76	2.1
AVG_{Sn}	94.63	99.49	4.86
AVG_{Sp}	98.68	99.85	1.17
AVG_{Pr}	96.37	99.55	3.18
AVG_{F1}	95.34	99.51	4.17

TABLE 7. Summary of the classification results obtained for the CNN and MPA-CNN on the INCART dataset.

Measures	CNN(%)	MPA-CNN(%)	Improvement(%)
AVG_{Acc}	93.83	99.47	5.60
AVG_{Sn}	87.14	98.89	12.69
AVG_{Sp}	96.87	99.66	2.76
AVG_{Pr}	88.17	98.99	10.73
AVG_{F1}	87.43	94.44	11.43

Tables 5, 6, and 7 present improvements for the MPA-CNN model over the CNN model without parameter optimization. MPA-CNN improves AVG_{Acc} with 5.37%, 2.1%, and 5.60% over MIT-BIH, EDB, and INCART respectively. Besides the model enhances AVG_{Sn} by 11.58%, 3.28%, and 12.69% over MIT-BIH,EDB, and INCART respectively.

B. COMPARATIVE STUDY

We compared the applicable dataset, feature extraction technique, classification models, and classification results with those of the existing studies. The results presented in the literature include the recognition of only five (four known and one unknown) classes as shown in Table 8. The proposed approach offers (on average) a 99.31%, 99.76%, and 99.47% increase in accuracy over the MIT-BIH, EDB, and INCART datasets, respectively. In terms of ACC and Sn, the highest accuracy is obtained for MPA-CNN. The results showed that the proposed approach produces significant performance improvement in the classification measurement factors compared with other approaches. Moreover, the results shown in the table 8 confirm the proposed model effectiveness.

VI. CONCLUSION

This paper proposes an ECG classification approach called MPA-CNN, which is based on parameters optimization of CNN using the MPA algorithm. The classification can

TABLE 8. Summary of comparisons between the proposed model and the existing methods.

Reference	classes	beats	Features	Classifier	Acc	Sn
[65]	5	34,989	Bispectrum PCA	SVM	93.48%	99.27%
[61]	5	83,648	End-to-end	CNN	99.00%	93.90%
[66]	5	1,800	DWT kernel ICA PCA	SVM	97.30%	97.40%
[67]	5	109,449	End-to-end	CNN	94.03%	96.71%
[68]	4	100,688	WPE, RR	RF	94.61%	98.50%
[69]	5	16,499	End-to-end	LSTM CNN	98.1%	97.5%
[70]	4	109,449	Fuzzy Entropy	KNN	98%	85.33%
[11]	4	94,013	End-to-end	31-layer deep ResNet	99.06%	93.21%
[71]	5	3,551	Fiducial points	PSO, GA, SVM, and RF	95.3%	94%
[72]	4	110,000	LBP,DWT, and Fiducial points	MRFO-SVM	98.26%	97.43%
Proposed	4	80,000	RR, LBP, HOS, and HPF	MPA-CNN	99.76%	99.49%

be implemented as follows: 1) To improve the predictive power of models considering heart problems, this analysis can be implemented with very large and different datasets. 2) Real-time surveillance of cardiac patients is essential for developing efficient methods for feature extraction and classification. 3) This study uses powerful classification models. For meaningful classification outcomes with improved accuracy, these models perform very well with the MPA algorithm and can enhance the accuracy of the classification process. 4) The results agree with those of previous studies. However, the results presented in the scientific literature include the classification classes in the AAMI standard. The MPA-CNN approach is faster and yields more accurate results than most existing techniques. The average detection accuracy levels for MPA with CNN classifier are 99.31% (MIT-BIH), 99.76% (EDB), and 99.47% (INCART). This suggests that the MPA algorithm is a more efficient and effective algorithm to obtain an optimized ECG classification model compared to other algorithms. It is worth exploring integrating the MPA with other machine learning classifiers as future research directions to optimize searching parameters of these classifiers for efficient detection of arrhythmia and heart rate abnormalities and failure.

DECLARATION OF COMPETING INTEREST

The authors declare that they have no known competing financial interests or personal relationships that could have appeared to influence the work reported in this paper.

AUTHOR CONTRIBUTIONS

All authors contributed equally to this paper, where Essam H. Houssein participated in sorting the experiments, discussed, analyzed the results, and revised/edited the manuscript. Ibrahim E. Ibrahim: performed the experiments and analyzed the results and wrote the paper. Diaa Salama AbdElminaam: discussed the results and wrote the paper.

Yaser M. Wazery: discussed the results and revised the paper. M. Hassaballah: analyzed the results and revised the paper. All authors approved the work in this paper.

REFERENCES

[1] J. Zhang, A. Liu, M. Gao, X. Chen, X. Zhang, and X. Chen, "ECG-based multi-class arrhythmia detection using spatio-temporal attention-based convolutional recurrent neural network," *Artif. Intell. Med.*, vol. 106, Jun. 2020, Art. no. 101856.

[2] Z. Ebrahimi, M. Loni, M. Daneshtalab, and A. Gharehbaghi, "A review on deep learning methods for ECG arrhythmia classification," *Expert Syst. Appl., X*, vol. 7, Sep. 2020, Art. no. 100033.

[3] B.-H. Kim and J.-Y. Pyun, "ECG identification for personal authentication using LSTM-based deep recurrent neural networks," *Sensors*, vol. 20, no. 11, p. 3069, May 2020.

[4] F. Liu, X. Zhou, J. Cao, Z. Wang, H. Wang, and Y. Zhang, "Arrhythmias classification by integrating stacked bidirectional LSTM and two-dimensional CNN," in *Proc. Pacific-Asia Conf. Knowl. Discovery Data Mining.* Cham, Switzerland: Springer, 2019, pp. 136–149.

[5] M. Abdi, A. Karimi, M. Navidbakhsh, G. P. Jahromi, and K. Hassani, "A lumped parameter mathematical model to analyze the effects of tachycardia and bradycardia on the cardiovascular system," *Int. J. Numer. Model., Electron. Netw., Devices Fields*, vol. 28, no. 3, pp. 346–357, May 2015.

[6] M. Hammad, S. Zhang, and K. Wang, "A novel two-dimensional ECG feature extraction and classification algorithm based on convolution neural network for human authentication," *Future Gener. Comput. Syst.*, vol. 101, pp. 180–196, Dec. 2019.

[7] W. Yang, Y. Si, D. Wang, and B. Guo, "Automatic recognition of arrhythmia based on principal component analysis network and linear support vector machine," *Comput. Biol. Med.*, vol. 101, pp. 22–32, Oct. 2018.

[8] A. Amirshahi and M. Hashemi, "ECG classification algorithm based on STDP and R-STDP neural networks for real-time monitoring on ultra low-power personal wearable devices," *IEEE Trans. Biomed. Circuits Syst.*, vol. 13, no. 6, pp. 1483–1493, Dec. 2019.

[9] P. Pławiak and U. R. Acharya, "Novel deep genetic ensemble of classifiers for arrhythmia detection using ECG signals," *Neural Comput. Appl.*, vol. 32, no. 15, pp. 11137–11161, Aug. 2020.

[10] R. Jothiramalingam, A. Jude, R. Patan, M. Ramachandran, J. H. Duraisamy, and A. H. Gandomi, "Machine learning-based left ventricular hypertrophy detection using multi-lead ECG signal," *Neural Comput. Appl.*, vol. 33, no. 9, pp. 4445–4455, May 2021.

[11] Z. Li, D. Zhou, L. Wan, J. Li, and W. Mou, "Heartbeat classification using deep residual convolutional neural network from 2-lead electrocardiogram," *J. Electrocardiol.*, vol. 58, pp. 105–112, Jan. 2020.

[12] T. F. Romdhane, H. Alhichri, R. Ouni, and M. Atri, "Electrocardiogram heartbeat classification based on a deep convolutional neural network and focal loss," *Comput. Biol. Med.*, vol. 123, Aug. 2020, Art. no. 103866.

[13] G. Sannino and G. De Pietro, "A deep learning approach for ECG-based heartbeat classification for arrhythmia detection," *Future Gener. Comput. Syst.*, vol. 86, pp. 446–455, Sep. 2018.

[14] M. Engin, "ECG beat classification using neuro-fuzzy network," *Pattern Recognit. Lett.*, vol. 25, no. 15, pp. 1715–1722, Nov. 2004.

[15] C. K. Roopa and B. S. Harish, "Automated ECG analysis for localizing thrombus in culprit artery using rule based information fuzzy network," *Int. J. Interact. Multimedia Artif. Intell.*, vol. 6, no. 1, p. 16, 2020.

[16] S. Edla, N. Kovvali, and A. Papandreou-Suppappola, "Electrocardiogram signal modeling with adaptive parameter estimation using sequential Bayesian methods," *IEEE Trans. Signal Process.*, vol. 62, no. 10, pp. 2667–2680, May 2014.

[17] K. Polat and S. Güneş, "Detection of ECG arrhythmia using a differential expert system approach based on principal component analysis and least square support vector machine," *Appl. Math. Comput.*, vol. 186, no. 1, pp. 898–906, Mar. 2007.

[18] V.-E. Neagoe, I.-F. Iatan, and S. Grunwald, "A neuro-fuzzy approach to classification of ECG signals for ischemic heart disease diagnosis," in *Proc. MIA Annu. Symp.*, 2003, p. 494.

[19] J. Lee, B. A. Reyes, D. D. Mcmanus, O. Maitas, and K. H. Chon, "Atrial fibrillation detection using an iPhone 4S," *IEEE Trans. Biomed. Eng.*, vol. 60, no. 1, pp. 203–206, Jan. 2013.

[20] E. H. Houssein, A. G. Gad, K. Hussain, and P. N. Suganthan, "Major advances in particle swarm optimization: Theory, analysis, and application," *Swarm Evol. Comput.*, vol. 63, Jun. 2021, Art. no. 100868.

[21] F. A. Hashim, E. H. Houssein, M. S. Mabrouk, W. Al-Atabany, and S. Mirjalili, "Henry gas solubility optimization: A novel physics-based algorithm," *Future Gener. Comput. Syst.*, vol. 101, pp. 646–667, Dec. 2019.

[22] E. H. Houssein, N. Neggaz, M. E. Hosney, W. M. Mohamed, and M. Hassaballah, "Enhanced Harris hawks optimization with genetic operators for selection chemical descriptors and compounds activities," *Neural Comput. Appl.*, vol. 102, pp 1–18, Apr. 2021.

[23] E. H. Houssein, M. E. Hosney, D. Oliva, W. M. Mohamed, and M. Hassaballah, "A novel hybrid harris hawks optimization and support vector machines for drug design and discovery," *Comput. Chem. Eng.*, vol. 133, Feb. 2020, Art. no. 106656.

[24] D. S. A. Elminaam, A. Nabil, S. A. Ibraheem, and E. H. Houssein, "An efficient marine predators algorithm for feature selection," *IEEE Access*, vol. 9, pp. 60136–60153, 2021.

[25] E. H. Houssein, D. S. Abdelminaam, H. N. Hassan, M. M. Al-Sayed, and E. Nabil, "A hybrid barnacles mating optimizer algorithm with support vector machines for gene selection of microarray cancer classification," *IEEE Access*, vol. 9, pp. 64895–64905, 2021.

[26] E. H. Houssein, B. E.-D. Helmy, A. A. Elngar, D. S. Abdelminaam, and H. Shaban, "An improved tunicate swarm algorithm for global optimization and image segmentation," *IEEE Access*, vol. 9, pp. 56066–56092, 2021.

[27] S. Deb, D. S. Abdelminaam, M. Said, and E. H. Houssein, "Recent methodology-based gradient-based optimizer for economic load dispatch problem," *IEEE Access*, vol. 9, pp. 44322–44338, 2021.

[28] D. S. Abdelminaam, M. Said, and E. H. Houssein, "Turbulent flow of water-based optimization using new objective function for parameter extraction of six photovoltaic models," *IEEE Access*, vol. 9, pp. 35382–35398, 2021.

[29] S. Deb, E. H. Houssein, M. Said, and D. S. Abdelminaam, "Performance of turbulent flow of water optimization on economic load dispatch problem," *IEEE Access*, vol. 9, pp. 77882–77893, 2021.

[30] W. H. El-Ashmawi, D. S. A. Elminaam, A. M. Nabil, and E. Eldesouky, "A chaotic owl search algorithm based bilateral negotiation model," *Ain Shams Eng. J.*, vol. 11, no. 4, pp. 1163–1178, Dec. 2020.

[31] D. S. Abdul-Minaam, W. M. E. S. Al-Mutairi, M. A. Awad, and W. H. El-Ashmawi, "An adaptive fitness-dependent optimizer for the one-dimensional bin packing problem," *IEEE Access*, vol. 8, pp. 97959–97974, 2020.

[32] W. H. El-Ashmawi and D. S. A. Elminaam, "A modified squirrel search algorithm based on improved best fit heuristic and operator strategy for bin packing problem," *Appl. Soft Comput.*, vol. 82, Sep. 2019, Art. no. 105565.

[33] D. S. Abdelminaam, F. H. Ismail, M. Taha, A. Taha, E. H. Houssein, and A. Nabil, "CoAID-DEEP: An optimized intelligent framework for automated detecting COVID-19 misleading information on Twitter," *IEEE Access*, vol. 9, pp. 27840–27867, 2021.

[34] D. S. AbdELminaam, A. M. Almansori, M. Taha, and E. Badr, "A deep facial recognition system using computational intelligent algorithms," *PLoS ONE*, vol. 15, no. 12, Dec. 2020, Art. no. e0242269.

[35] D. S. Abdul and S. A. Ibrahim, "Building a robust heart diseases diagnose intelligent model based on RST using LEM2 and MODLEM2," in *Proc. 32nd Int. Bus. Inf. Manage. Assoc. Conf. (IBIMA)*, 2018, pp. 5733–5744.

[36] C. Sridhar, U. R. Acharya, H. Fujita, and G. M. Bairy, "Automated diagnosis of coronary artery disease using nonlinear features extracted from ECG signals," in *Proc. IEEE Int. Conf. Syst., Man, Cybern. (SMC)*, Oct. 2016, pp. 000545–000549.

[37] P. Kora, A. Abraham, and K. Meenakshi, "Heart disease detection using hybrid of bacterial foraging and particle swarm optimization," *Evolving Syst.*, vol. 11, no. 1, pp. 15–28, Mar. 2020.

[38] B. Navaneeth and M. Suchetha, "PSO optimized 1-D CNN-SVM architecture for real-time detection and classification applications," *Comput. Biol. Med.*, vol. 108, pp. 85–92, May 2019.

[39] M. Zubair, J. Kim, and C. Yoon, "An automated ECG beat classification system using convolutional neural networks," in *Proc. 6th Int. Conf. IT Converg. Secur. (ICITCS)*, Sep. 2016, pp. 1–5.

[40] S. Nurmaini, R. U. Partan, W. Caesarendra, T. Dewi, M. N. Rahmatullah, A. Darmawahyuni, V. Bhayyu, and F. Firdaus, "An automated ECG beat classification system using deep neural networks with an unsupervised feature extraction technique," *Appl. Sci.*, vol. 9, no. 14, p. 2921, Jul. 2019.

[41] C. Chen, Z. Hua, R. Zhang, G. Liu, and W. Wen, "Automated arrhythmia classification based on a combination network of CNN and LSTM," *Biomed. Signal Process. Control*, vol. 57, Mar. 2020, Art. no. 101819.

[42] S. Raj and K. C. Ray, "Sparse representation of ECG signals for automated recognition of cardiac arrhythmias," *Expert Syst. Appl.*, vol. 105, pp. 49–64, Sep. 2018.

[43] G. Wang, C. Zhang, Y. Liu, H. Yang, D. Fu, H. Wang, and P. Zhang, "A global and updatable ECG beat classification system based on recurrent neural networks and active learning," *Inf. Sci.*, vol. 501, pp. 523–542, Oct. 2019.

[44] Q. Yao, R. Wang, X. Fan, J. Liu, and Y. Li, "Multi-class arrhythmia detection from 12-lead varied-length ECG using attention-based time-incremental convolutional neural network," *Inf. Fusion*, vol. 53, pp. 174–182, Jan. 2020.

[45] K. Kærgaard, S. H. Jensen, and S. Puthusserypady, "A comprehensive performance analysis of EEMD-BLMS and DWT-NN hybrid algorithms for ECG denoising," *Biomed. Signal Process. Control*, vol. 25, pp. 178–187, Mar. 2016.

[46] R. R. Sharma and R. B. Pachori, "Baseline wander and power line interference removal from ECG signals using eigenvalue decomposition," *Biomed. Signal Process. Control*, vol. 45, pp. 33–49, Aug. 2018.

[47] Y. Kaya, M. Uyar, R. Tekin, and S. Yıldırım, "1D-local binary pattern based feature extraction for classification of epileptic EEG signals," *Appl. Math. Comput.*, vol. 243, pp. 209–219, Sep. 2014.

[48] J. R. Annam, S. Kalyanapu, S. Ch., J. Somala, and S. B. Raju, "Classification of ECG heartbeat arrhythmia: A review," *Procedia Comput. Sci.*, vol. 171, pp. 679–688, Jan. 2020.

[49] L. B. Marinho, N. D. M. M. Nascimento, J. W. M. Souza, M. V. Gurgel, P. P. R. Filho, and V. H. C. de Albuquerque, "A novel electrocardiogram feature extraction approach for cardiac arrhythmia classification," *Future Gener. Comput. Syst.*, vol. 97, pp. 564–577, Aug. 2019.

[50] N. M. M. Nascimento, L. B. Marinho, S. A. Peixoto, J. P. do Vale Madeiro, V. H. C. de Albuquerque, and P. P. R. Filho, "Heart arrhythmia classification based on statistical moments and structural co-occurrence," *Circuits, Syst., Signal Process.*, vol. 39, no. 2, pp. 631–650, Feb. 2020.

[51] I. Daubechies and W. Sweldens, "Factoring wavelet transforms into lifting steps," *J. Fourier Anal. Appl.*, vol. 4, no. 3, pp. 247–269, May 1998.

[52] N. Japkowicz, "The class imbalance problem: Significance and strategies," in *Proc. Int. Conf. Artif. Intell.*, vol. 56, 2000, pp. 1–7.

[53] P. Radivojac, N. V. Chawla, A. K. Dunker, and Z. Obradovic, "Classification and knowledge discovery in protein databases," *J. Biomed. Informat.*, vol. 37, no. 4, pp. 224–239, Aug. 2004.

[54] Z. Zheng, X. Wu, and R. Srihari, "Feature selection for text categorization on imbalanced data," *ACM SIGKDD Explor. Newslett.*, vol. 6, no. 1, pp. 80–89, Jun. 2004.

[55] E. H. Houssein, M. Kilany, and A. E. Hassanien, "ECG signals classification: A review," Int. J. Intell. Eng. Inform., vol. 5, no. 4, pp. 376–396, 2017.

[56] N. V. Chawla, K. W. Bowyer, L. O. Hall, and W. P. Kegelmeyer, "SMOTE: Synthetic minority over-sampling technique," J. Artif. Intell. Res., vol. 16, pp. 321–357, Jun. 2002.

[57] P. De Chazal, M. O'Dwyer, and R. B. Reilly, "Automatic classification of heartbeats using ECG morphology and heartbeat interval features," IEEE Trans. Biomed. Eng., vol. 51, no. 7, pp. 1196–1206, Jul. 2004.

[58] T. Mar, S. Zaunseder, J. P. Martínez, M. Llamedo, and R. Poll, "Optimization of ECG classification by means of feature selection," IEEE Trans. Biomed. Eng., vol. 58, no. 8, pp. 2168–2177, Aug. 2011.

[59] M. Llamedo and J. P. Martínez, "Heartbeat classification using feature selection driven by database generalization criteria," IEEE Trans. Biomed. Eng., vol. 58, no. 3, pp. 616–625, Mar. 2011.

[60] P. De Chazal and R. B. Reilly, "A patient-adapting heartbeat classifier using ECG morphology and heartbeat interval features," IEEE Trans. Biomed. Eng., vol. 53, no. 12, pp. 2535–2543, Dec. 2006.

[61] S. Kiranyaz, T. Ince, and M. Gabbouj, "Real-time patient-specific ECG classification by 1-D convolutional neural networks," IEEE Trans. Biomed. Eng., vol. 63, no. 3, pp. 664–675, Mar. 2016.

[62] A. Faramarzi, M. Heidarinejad, S. Mirjalili, and A. H. Gandomi, "Marine predators algorithm: A nature-inspired Metaheuristic," Expert Syst. Appl., vol. 152, Aug. 2020, Art. no. 113377.

[63] E. H. Houssein, M. R. Saad, F. A. Hashim, H. Shaban, and M. Hassaballah, "Lévy flight distribution: A new metaheuristic algorithm for solving engineering optimization problems," Eng. Appl. Artif. Intell., vol. 94, Sep. 2020, Art. no. 103731.

[64] J. D. Filmalter, L. Dagorn, P. D. Cowley, and M. Taquet, "First descriptions of the behavior of silky sharks, Carcarhinus falciformis, around drifting fish aggregating devices in the Indian Ocean," Bull. Mar. Sci., vol. 87, no. 3, pp. 325–337, Jul. 2011.

[65] R. J. Martis, U. R. Acharya, K. M. Mandana, A. K. Ray, and C. Chakraborty, "Cardiac decision making using higher order spectra," Biomed. Signal Process. Control, vol. 8, no. 2, pp. 193–203, Mar. 2013.

[66] H. Li, D. Yuan, Y. Wang, D. Cui, and L. Cao, "Arrhythmia classification based on multi-domain feature extraction for an ECG recognition system," Sensors, vol. 16, no. 10, p. 1744, 2016.

[67] U. R. Acharya, S. L. Oh, Y. Hagiwara, J. H. Tan, M. Adam, A. Gertych, and R. S. Tan, "A deep convolutional neural network model to classify heartbeats," Comput. Biol. Med., vol. 89, pp. 389–396, Oct. 2017.

[68] T. Li and M. Zhou, "ECG classification using wavelet packet entropy and random forests," Entropy, vol. 18, no. 8, p. 285, Aug. 2016.

[69] S. L. Oh, E. Y. K. Ng, R. S. Tan, and U. R. Acharya, "Automated diagnosis of arrhythmia using combination of CNN and LSTM techniques with variable length heart beats," Comput. Biol. Med., vol. 102, pp. 278–287, Nov. 2018.

[70] M. Sharma, R.-S. Tan, and U. R. Acharya, "Automated heartbeat classification and detection of arrhythmia using optimal orthogonal wavelet filters," Informat. Med. Unlocked, vol. 16, Jan. 2019, Art. no. 100221.

[71] K. K. Patro, A. J. Prakash, M. J. Rao, and P. R. Kumar, "An efficient optimized feature selection with machine learning approach for ECG biometric recognition," IETE J. Res., vol. 2020, pp. 1–12, Feb. 2020.

[72] E. H. Houssein, I. E. Ibrahim, N. Neggaz, M. Hassaballah, and Y. M. Wazery, "An efficient ECG arrhythmia classification method based on manta ray foraging optimization," Expert Syst. Appl., vol. 181, Nov. 2021, Art. no. 115131.

DIAA SALAMA ABDELMINAAM received the Ph.D. degree in information system from the Faculty of Computers and Information, Menufia university, Egypt, in 2015. He is currently an Assistance Professor with the Department of Information Systems, Faculty of Computers and Information, Benha University, Egypt. He has worked on several research topics. He has contributed more than 40 technical articles in the areas of wireless networks, wireless network security, information security and Internet applications, cloud computing, mobile cloud computing, the Internet of Things, and machine learning in international journals and conferences. His major interests include cryptography, network security, the IoT, big data, cloud computing, and deep learning.

IBRAHIM E. IBRAHIM is currently pursuing the M.Sc. degree in information technology with the Faculty of Computers and Information, Minia University, Egypt. He is also a full-time Teaching Assistant with the Faculty of Computers and Information, Luxor University, Egypt. He is a member of the Computing and Artificial Intelligence Research Group (CAIRG), Egypt. His research interests include cloud computing, scheduling, the IoT, machine learning, data mining, and optimization.

M. HASSABALLAH received the B.Sc. degree in mathematics and the M.Sc. degree in computer science from South Valley University, Egypt, in 1997 and 2003, respectively, and the D.Eng. degree in computer science from Ehime University, Japan, in 2011. He was a Visiting Scholar with the Department of Computer and Communication Science, Wakayama University, Japan, in 2013, and the GREAH Laboratory, Le Havre Normandie University, France, in 2019. He is currently an Associate Professor of computer science with the Department of Computer Science, Faculty of Computers and Information, South Valley University. He has published five books and over 60 research articles in refereed international journals and over 60 research papers in refereed international conferences. His research interests include artificial intelligence, computer vision, image processing, biometrics, feature extraction, object detection/recognition, machine learning, and data hiding. He serves as a Reviewer for several journals, such as IEEE TRANSACTIONS ON IMAGE PROCESSING, IEEE TRANSACTIONS ON CIRCUITS AND SYSTEMS FOR VIDEO TECHNOLOGY, IEEE TRANSACTIONS ON INDUSTRIAL INFORMATICS, IEEE TRANSACTIONS ON FUZZY SYSTEMS, Neurocomputing, Pattern Recognition, Pattern Recognition Letters, IET Image Processing, IET Computer Vision, IET Biometrics, Journal of Real-Time Image Processing, and The Computer Journal. He is an Editorial Board Member of Pattern Analysis and Applications, IET Image Processing and Wireless Communications and Mobile Computing journals. He serves as a TPC member for many conferences.

ESSAM H. HOUSSEIN received the Ph.D. degree in computer science in 2012. He is currently an Associate Professor with the Faculty of Computers and Information, Minia University, Egypt. He is also the Founder and the Chair of the Computing and Artificial Intelligence Research Group (CAIRG), Egypt. He has more than 100 scientific research articles published in prestigious international journals in the topics for instance meta-heuristics optimization, artificial intelligence, image processing, and the IoT and its applications. His research interests include WSNs, the IoT, AI, bioinformatics and biomedical, image processing, data mining, and meta-heuristics optimization techniques. He serves as a Reviewer of more than 40 journals, such as Elsevier, Springer, and IEEE.

YASER M. WAZERY received the Ph.D. degree in information technology. He is currently an Associate Professor with the Department of Information Technology, Faculty of Computers and Information, Minia University, Egypt. His main research interests include network security, cryptography, biological inspired clustering, multimedia communications and processing, big data, cloud computing, and data mining.